Published as: *Environ Sci Technol*. 2008 April 1; 42(7): 2380–2386.

Redox Reactions of Phenazine Antibiotics with Ferric (Hydr) oxides and Molecular Oxygen

Yun Wang[†] and **Dianne K. Newman**[*,†,‡]

[†]Department of Biology, Massachusetts Institute of Technology, 77 Massachusetts Avenue, Cambridge, Massachusetts 02139

[‡]Department of Earth, Atmospheric and Planetary Sciences, Massachusetts Institute of Technology, 77 Massachusetts Avenue, Cambridge, Massachusetts 02139

Abstract

Phenazines are small redox-active molecules produced by a variety of bacteria. Beyond merely serving as antibiotics, recent studies suggest that phenazines play important physiological roles, including one in iron acquisition. Here we characterize the ability of four electrochemically reduced natural phenazines—pyocyanin (PYO), phenazine-1-carboxylate (PCA), phenazine-1-carboxamide, and 1-hydroxyphenazine (1-OHPHZ)—to reductively dissolve ferrihydrite and hematite in the pH range 5–8. Generally, the reaction rate is higher for a phenazine with a lower reduction potential, with the reaction between PYO and ferrihydrite at pH 5 being an exception; the rate decreases as the pH increases; the rate is higher for poorly crystalline ferrihydrite than for highly crystalline hematite. Ferric (hydr)oxide reduction by reduced phenazines can potentially be inhibited by oxygen, where O_2 competes with Fe(III) as the final oxidant. The reactivity of reduced phenazines with O_2 decreases in the order: PYO > 1-OHPHZ > PCA. Strikingly, reduced PYO, which is the least reactive phenazine with ferrihydrite and hematite at pH 7, is the most reactive phenazine with O_2. These results imply that different phenazines may perform different functions in environments with gradients of iron and O_2.

Introduction

In most aerobic environments, iron is present as insoluble Fe(III) minerals. Microbially mediated Fe(III) reduction plays important roles in a variety of biogeochemical cycles (including C, N, O, P, and many metals) and in the degradation of organic and inorganic contaminants in diverse aquatic settings (1). Fe(III) reduction is also important in bacterial physiology with respect to mineral respiration (1), as well as iron acquisition by providing soluble and, hence, bioavailable Fe(II) (2). While *Geobacter* species require direct contact with Fe(III) minerals via outer membrane c-type cytochromes (3) or highly conductive pili (4) to reduce Fe(III), many other bacteria, including *Pseudomonas*, *Shewanella*, and *Geothrix* species, can indirectly reduce Fe(III) via exogenous and/or endogenous electron shuttles (5–9). Electron shuttles are redox-active small molecules that are reduced within the bacterial cell and are oxidized outside the cell by terminal electron acceptors such as Fe(III) minerals and molecular oxygen (10,11). Given enough terminal electron acceptors, one shuttle molecule can

*Corresponding author dkn@mit.edu; phone: 617-324-2770; fax: 617-324-3972.

Supporting Information Available

Detailed descriptions of phenazine purification, ferric (hydr) oxides preparation, lists of initial rates, plots from cyclic voltammetry experiments, Eh-pH diagrams, characteristic UV–visible spectra of phenazines, Fe(II) adsorption plots, illustrative time course for reaction of the reduced phenazine with O_2. This information is available free of charge via the Internet at http://pubs.acs.org.

be recycled many times. This shuttling process is thought to be especially important in a biofilm environment where a terminal electron acceptor is not easily accessible, because it is either insoluble (e.g., Fe(III) minerals) or diffusion-limited (e.g., O_2) (10).

Humic substances and their analogue anthraquinone-2,6-disulfonate (2,6-AQDS) are exogenous electron shuttles for Fe(III) reduction, where the redox-active moieties are quinone groups (5,12). Phenazines are endogenous redox-active molecules with heterocyclic ring structures that are functionally similar to those of humic substances and 2,6-AQDS. They are produced by *Pseudomonas* species and a few other bacterial genera, including soil and clinical isolates (13). Like other electron shuttles, phenazines often have reduction potentials sufficiently low under common physiological and environmental conditions so that the redox reactions between reduced phenazines and terminal electron acceptors such as Fe(III) are thermodynamically feasible (6,10,11). Early studies showed that phenazines can promote microbial Fe(III) reduction from transferrin-bound Fe(III) (14) and poorly crystalline Fe(III) (hydr)oxide (6). Moreover, results from genetic analyses suggest phenazine production may facilitate iron acquisition (15). Although various reductants can reduce Fe(III) minerals with the reductants being irreversibly oxidized (16), here we focus on Fe(III) reductive dissolution that is stimulated by phenazine electron shuttles.

Fe(III) mineral reduction by reduced phenazines potentially can be inhibited by oxygen, where O_2 competes with Fe(III) as the final oxidant. Therefore, it makes sense that phenazine production is stimulated by low oxygen tension and the presence of Fe(III) in certain isolates (17,18), a condition that seems to favor Fe(III) mineral reduction. In addition, when *P. aeruginosa* grows anaerobically, pyocyanin (PYO) production is completely inhibited, but production of phenazine-1-carboxylate (PCA) is allowed (15,19). Why is phenazine production influenced by environmental factors like O_2 and Fe(III)? Can different phenazines preferentially react with Fe(III) over O_2, or vice versa? Phenazines come in different structures with different redox properties. Here we investigate whether it is possible to predict phenazine reactivity based on their structural characteristics by studying the redox reactions of four electrochemically reduced endogenous phenazines with Fe(III) (hydr)oxides and O_2. In addition, we explore the influence of pH and Fe(III) mineralogy on their reactivity.

Materials and Methods

Chemicals

All solutions were prepared from reagent grade chemicals without further purification, and distilled, deionized water (DDW) with a resistivity of 18 MΩ-cm. 1,10-Phenanthroline, hydroxylamine hydrochloride, trifluoroacetic acid(TFA), acetonitrile, 3-(*n*-morpholino) propanesulfonic acid (MOPS), EDTA, $Fe(NO_3)_3 \cdot 9H_2O$, and KOH were purchased from Sigma-Aldrich. Ammonium acetate ($CH_3C(O)\text{-}ONH_4$) was purchased from Fluka. 1-Hydroxyphenazine (1-OHPHZ, oxidized form) was purchased from TCI America.

Three phenazines—PYO, PCA, and phenazine-1-carbox-amide (PCN)—were purified from aerobic bacterial cultures (see Supporting Information for details). The purified phenazines were present in their oxidized form and were dissolved in 0.1 M KCl aqueous solutions buffered with 10 mM $CH_3C(O)ONH_4$-MOPS (5 mM each, pH 7) to yield stock solution concentrations of 829 μM for PYO, 1.34 mM for PCA, and 68 μM for PCN.

Electrochemical Experiments

Electrochemical measurements were performed with a Gamry PC4–300 potentiostat. All experiments were conducted in an O_2-free glovebox (Coy Laboratory Products) and in the dark. All measured potentials were referenced to a Ag/AgCl electrode (RE-5B, BASi).

Reported potentials were referenced to the normal hydrogen electrode (NHE) (V vs NHE = V vs Ag/AgCl + 207 mV) to permit comparisons with other studies. The half-wave potentials ($E_{1/2}$) of each phenazine at different pHs (pH 5, 6, 7, and 8) were determined using cyclic voltammetry (CV) in 0.1 M KCl buffered with 10 mM $CH_3C(O)ONH_4$-MOPS in a one-compartment cell. The pH was adjusted by adding HCl or NaOH. A stationary gold disk electrode (BASi) was used as the working electrode, and a straight platinum wire (BASi) was the counter electrode. Scans were performed between 20 and 500 mV/s in the potential range of around $E_{1/2} \pm 0.3$ (V).

The reduced form of each phenazine was obtained using controlled potential bulk electrolysis in 0.1 M KCl buffered with 10 mM $CH_3C(O)ONH_4$-MOPS at pH 7. A high surface area reticulated vitreous carbon electrode (BASi) was used as the working electrode, and a coiled platinum wire (BASi) was the counter electrode. A two-compartment cell was used for bulk electrolysis. The working electrode was in a sample compartment together with the reference electrode. The counter electrode was in another compartment isolated from the working electrode. The two compartments were joined by a fritted glass junction. The controlled potential bulk electrolysis was set 100–150 mV more negative than $E_{1/2}$ at pH 7 for each phenazine to perform a nearly complete reduction (98–99% being reduced). All electrolyses were terminated when the current fell below 2% of the initial current. The charge being transferred during the electrolysis was measured in the electrolyte both with and without phenazine. The net charge caused by phenazine reduction was calculated by subtracting the background electrolysis without phenazine being added. Linear sweep voltammetries (LSV) were performed before and after the bulk electrolysis of each phenazine, scanned from the potential $E_{1/2} + 0.3$ to $E_{1/2}-0.3$ V at 50 mV/s, using the working electrode for cyclic voltammetry, to confirm complete phenazine reduction.

Preparation of Ferric (Hydr)oxides

$Fe(OH)_3$(am, s) refers to the ferrihydrite particles synthesized according to the method described in Schwertmann and Cornell (20) (see Supporting Information for details). X-ray diffraction showed two broad peaks at 2.4 and 1.5 Å, consistent with the mineral 2-line ferrihydrite (20). Freeze-dried $Fe(OH)_3$(am, s) yielded a BET (Brunauer–Emmett–Teller) surface area of 312 m^2/g and weighed 108 g per mole of iron. α-Fe_2O_3(s), referring to the hematite particles synthesized according to the method described in Schwertmann and Cornell (20), was provided by Professor Scherer's group (University of Iowa). Morphology and *d*-spacings were consistent with the mineral hematite (20). Freeze-dried α-Fe_2O_3(s) yielded a BET surface area of 30 m^2/g and weighed 97.4 g per mole of iron. To verify that the Fe $(OH)_3$(am, s) and α-Fe_2O_3(s) were sterile, we inoculated the oxides in LB medium, incubated at 30 °C overnight, then plated the cultures onto 1.5% agar–LB plates and incubated at 30 °C for two days. No growth was observed on the plates, indicating the oxides were sterile.

Fe(II) Sorption Experiments

All experiments were conducted in the dark at 25 °C in an O_2-free glovebox. Reactions were initiated by mixing 100 μM of Fe(III) suspension, 5.0 mM $CH_3C(O)ONH_4$-MOPS (2.5 mM each compound), $FeCl_2$ solution, and DDW into 20 mL polypropylene bottles. The pH was adjusted by adding HCl and NaOH, and the solution was buffered by $CH_3C(O)ONH_4$-MOPS. Stirring was performed using Teflon-coated stir bars. Suspensions were equilibrated for 12 h prior to filtration through a 0.2 μm polycarbonate filter. Filtered solutions were analyzed for aqueous Fe(II) by the phenanthroline assay (21). The amount of adsorbed Fe(II) was calculated from the difference between total and aqueous Fe(II) in the suspension.

Redox Experiments between Reduced Phenazines and Ferric (Hydr)oxides

All batch experiments were conducted in 125 mL polypropylene bottles in the dark at 25 °C in an O_2-free glovebox and were stirred with Teflon-coated stir bars. To maintain constant pH from 5 to 8, 5.0 mM $CH_3C(O)ONH_4$-MOPS buffer was employed. The pH buffer concentration was high enough to maintain a constant ionic strength. No additional electrolyte was added. Reactions were initiated by adding $Fe(OH)_3$(am, s) or α-Fe_2O_3(s) into reaction solutions mixed together with pH buffer and reduced phenazine. Three milliliter reaction suspension aliquots were collected at periodic intervals. Reactions were quenched by immediately filtering through 0.2 μm filters. Dissolved Fe(II) in the filtrates was analyzed by the phenanthroline assay (22). Total dissolved Fe was also analyzed for some filtrates using ICP-MS. Phenazine oxidation was followed by the characteristic change of the adsorption spectrum accompanying the transformation from the reduced form to the oxidized form. To do this, the filtrates were transferred to VWR micro-UV cuvettes inside the glovebox and sealed with rubber stoppers, and the UV–visible spectra were recorded using a Beckman Coulter DU800 spectrophotometer outside the glovebox.

Redox Experiments between Reduced Phenazines and Oxygen

All experiments were conducted in 3.5 mL Starna fluorescence cuvettes at 25 °C and were stirred with Teflon-coated micro stir bars. The buffer solution consisting of 2.0% O_2 balanced with N_2, 1.0 mM phosphate (pH 7.0), and 100 μM EDTA was prepared in a stoppered serum bottle. EDTA was added to complex and subsequently quench side reactions caused by residual transition metal ions in the solution. Reduced phenazine stock solution was first transferred into a cuvette inside the glovebox. The cuvette was then sealed with a rubber septum and moved outside the glovebox so that reaction progress could be monitored. Next, the reaction was initiated by instantaneous mixing of the reactants upon injecting the O_2-containing buffer solution into the cuvette. The initial reaction condition was to have 5 μM reduced phenazine and 2.0% O_2 (27 μM). The change of initial O_2 concentration upon mixing was negligible because the concentrations of reduced phenazine stock solutions were much higher than 5 μM. Phenazine oxidation was followed by the characteristic fluorescence change accompanying transformation from the reduced form to the oxidized form. At the specific excitation/emission wavelength set, 329/492 nm for PYO, 395/566 nm for PCA, and 355/485 nm for 1-OHPHZ, only the reduced form fluoresces, not the oxidized form; hence, by using a Jobin Yvon SPEX Fluorolog-3-spectrofluorometer, a decrease in fluorescence intensity over time can be recorded for each reaction. Reaction with O_2 was not performed for PCN because the fluorescence of the oxidized vs reduced form cannot be differentiated.

Results and Discussion

Electrochemical Properties of Phenazines

Phenazines come in different forms with different redox properties. We measured the reduction potentials of four natural phenazines in aqueous electrolyte from pH 5 to 8 with CV analyses. Under most conditions, CVs of each phenazine exhibited single oxidation (anodic) and reduction (cathodic) peaks where the ratios of the anodic and cathodic peak currents were close to unity; the peak current increased linearly with the square root of the voltage scan rate; the peak potential was relatively independent of the voltage scan rate (Figure 1a, and Figure S1a in Supporting Information). These results indicate diffusion-controlled, reversible (Nernstian) electrode reactions (23), where the half-wave potentials ($E_{1/2}$) reported in Table 1, that is, the potential midways between anodic and cathodic peak potentials, are accurate representations of the formal reduction potentials under the same experimental condition (23). $E_{1/2}$ values for PCA and PCN at pH 8 cannot be reported because electrode reactions deviated from the Nernstian condition, probably due to side reactions such as sorption on the electrode surface.

The oxidation–reduction reactions of phenazines involve protons. The CV peaks of each phenazine shifted negatively as the pH was increased (Figure 1b), and $E_{1/2}$ shifted linearly with pH, giving a slope close to 59 mV/pH unit (Figure S1b, Supporting Information), indicating that each electron transferred was matched by one proton, based on the Nernst Equation:

$$E = E^0 + \frac{0.059}{n}\log\frac{[\mathrm{phz}]_{ox}[\mathrm{H}^+]^m}{[\mathrm{phz}]_{re}} = \left(E^0 + \frac{0.059}{n}\log\frac{[\mathrm{phz}]_{ox}}{[\mathrm{phz}]_{re}}\right) - \frac{0.059 \times m}{n}\mathrm{pH\ (V)} \quad (1)$$

For PCA, PCN, and 1-OHPHZ, the observed slope was expected and consistent with earlier studies (24, 25). The oxidized form of PYO has a pK_a at pH 4.9 (26), where protonation/deprotonation occurs without necessarily being coupled to electron transfer; hence, the slope is expected to deviate from 59 mV/pH unit at the pHs near the pK_a. Although an earlier study over a wide pH range observed a deviation near pH 4.9 (26), we did not observe it because the lowest pH we studied was pH 5.

Reduced phenazines were obtained by controlled potential bulk electrolysis at pH 7. Upon reduction, PYO turned from blue to colorless, PCA and PCN turned from pale yellow to bright yellow, and 1-OHPHZ turned from orange-yellow to colorless (Figure S2 for UV–visible spectra, Supporting Information). Reoxidizing each reduced phenazine with air yielded a single phenazine peak with the characteristic peak size in HPLC analyses, ruling out any irreversible degradation. The color changes upon electrochemical reduction were consistent with earlier studies employing chemical reduction followed by potentiometric titration (24–26), characteristic of two-electron reduction.

Together, these results indicate that, from pH 5 to 8, the electrochemical oxidation–reduction reactions of all four phenazines were two-electron, two-proton transfer coupled processes (Table 1). $E_{1/2}$ decreased in the order: PYO > PCA > PCN > 1-OHPHZ, ranging over 100 mV in potential difference. At pH7, all four phenazines exhibited negative $E_{1/2}$ values. $E_{1/2}$ for PYO and 1-OHPHZ were comparable with those reported by other groups (25,26), but our PCA and PCN measurements differed (24,27). This is likely because earlier studies added a high percentage of alcohol to increase PCA and PCN solubility (24,27); hence, they cannot be directly compared with our results obtained in aqueous solution.

Fe(II) Sorption

Iron(II) sorption experiments were performed to determine whether it is feasible to calculate rates based on aqueous Fe(II) (Fe(II)(aq)) production for redox reactions between reduced phenazines and Fe(III) (hydr)oxides, given that these rates are accurate only if Fe(II) sorption is low. For experiments employing a loading of 100 μM Fe(III), Fe(II) sorption on both $Fe(OH)_3$(am, s) and α-Fe_2O_3(s) was no higher than 1–2 μM at pH ≤ 7 and increased with pH > 7 (Figure S3, Supporting Information). The apparent sudden increase in Fe(II) “sorption” coinciding with raising the pH from 7 to 8, especially for $Fe(OH)_3$(am, s), implies that surface reactions other than simple sorption occur. Iron speciation calculations (Figure 1) and previous studies suggest that near-surface precipitates such as the mixed valent magnetite (28) or $Fe(OH)_2$(s) (22) may form above pH 7. Hence, rates determined based on Fe(II)(aq) production are accurate at pH 7 and lower.

Reactions with Ferric (Hydr)oxides: Time Course, Products, and Stoichiometry

Reduced phenazine-free blank suspensions containing a Fe(III) loading of 100 μM in the pH range 5–8 did not yield dissolved Fe concentrations (Fe_T) above the ICP-MS detection limit of 1–2 μM after 7 days of reaction. In all the experiments performed for reacting reduced phenazines with $Fe(OH)_3$(am, s) or α-Fe_2O_3(s), dissolved Fe(II) (Fe(II)(aq)) measured with

the phenanthroline assay and Fe_T measured with ICP-MS were consistently equal to one another, indicating reductive dissolution was dominant. All experiments with ferric (hydr) oxides employed 50 μM reduced phenazine and 100 μM of Fe(III). A typical time course exhibited the formation of Fe(II)(aq), the loss of reduced phenazine, and the formation of oxidized phenazine (Figure 2) as the reaction progressed. UV–visible spectra showed isosbestic points, indicating stoichiometric conversion of phenazine from the reduced to the oxidized form. By calculating the concentrations based on the molar extinction coefficients characteristic for the oxidized and/or reduced phenazines, we recovered the concentration of the total added phenazine from the redox-couples listed in Table 1. In HPLC analyses, filtered reaction solutions exposed to air only yielded a single phenazine peak with the characteristic peak size, ruling out phenazine oxidation via an irreversible degradation pathway.

The quantitative two-electron oxidation of phenazines versus one-electron reduction of ferric (hydr)oxide should yield the following reaction stoichiometry:

$$\text{With ferrihydrite: } H_2PHZ + 2Fe(OH)_3(\text{am, s}) + 4H^+ = 2Fe^{2+} + PHZ + 6H_2O \quad (2)$$

$$\text{With hemeatite: } H_2PHZ + \alpha\text{–}Fe_2O_3(s) + 4H^+ = 2Fe^{2+} + PHZ + 3H_2O \quad (3)$$

where H_2PHZ represents a reduced phenazine, and PHZ represents an oxidized phenazine. The measured ratios of Fe(II)(aq) formed versus phenazine oxidized were nearly 2:1 for experiments performed atpH 7 or lower, as expected. For experiments performed at pH 8, the ratios became lower, which may arise from a higher extent of Fe(II) sorption or precipitation.

Reactions with Ferric (Hydr)oxides: Thermodynamics

We constructed an Eh/pH diagram (Figure S4, Supporting Informtion) to assess under what conditions ferric (hydr)oxide reduction by reduced phenazines would be expected to be thermodynamically favorable. For iron speciation, we assumed the concentration of total dissolved Fe (Fe_T) to be 1 μM, and we neglected carbonate species for simplicity. For phenazine speciation, we assumed the ratio of the reduced versus the oxidized phenazine to be 100:1 to calculate the reduction potentials versus pH; the calculations from $E_{1/2}$ measured at different pH values (symbols) and the extrapolations from $E_{1/2}$ measured at pH 7 (dashed lines) were the same. Given these parameters, we predict that the reactions of reduced phenazines with ferric (hydr)oxides are more thermodynamically favorable at lower pH values. Compared to the poorly crystalline $Fe(OH)_3$(am, s), the highly crystalline α-Fe_2O_3(s) has a lower reduction potential (29); subsequently, its reactions with reduced phenazines are expected to occur at lower pH values. For example, reduction of $Fe(OH)_3$(am, s) by all four phenazines is thermodynamically favorable at pH 8; reduction of α-Fe_2O_3(s), on the other hand, becomes thermodynamically unfavorable at pH 7 or higher for three of the four phenazines (1-OHPHZ being the exception). Phenazines with lower reduction potentials are expected to reduce ferric (hydr)oxides at higher pH. For example, reduction of ferric (hydr)oxides by PYO occurs at lower pH values than for other phenazines because PYO has a higher reduction potential. For a given phenazine and ferric (hydr)oxide, from the Nernst equation, the lower the amount of Fe^{2+}(aq) present in the system, the more likely the redox reaction will occur at a higher pH. In addition, the greater the ratio of reduced-to-oxidized phenazines, the more favorable the redox reaction will be at a higher pH and/or higher Fe^{2+}(aq) concentrations.

Reactions with Ferric (Hydr)oxides: Kinetics

To make reactivity comparisons, we determined initial rates with respect to Fe(II)(aq) production for reactions of reduced phenazines with $Fe(OH)_3$(am, s) and α-Fe_2O_3(s) from pH 5 to 8 (Table S1, Supporting Information), based on the method previously described (30). R_0 (μM/h) was obtained directly from the slopes of concentration versus time plots (Figure 2a). R_A (μmole m^{-2} h^{-1}), the area-corrected rate, was obtained to compare (hydr)oxides with different surface areas.

To assess whether correlations exist between the reaction kinetics and phenazine thermodynamic properties, we plotted the logarithms of the initial rates against the half-wave potentials ($E_{1/2}$) of the phenazine redox couples (Figure 3). For reactions with $Fe(OH)_3$(am, s), the log R was associated but not linearly correlated with the phenazine $E_{1/2}$. 1-OHPHZ, the phenazine with the lowest $E_{1/2}$, yielded the highest rate at all four pH values (5, 6, 7, and 8). PCA and PCN yielded similar rates, consistent with their similar $E_{1/2}$ values. PYO, the phenazine with the highest $E_{1/2}$, failed to yield a measurable rate at pH 7 and 8, in contrast to the other phenazines. However, PYO became highly reactive with $Fe(OH)_3$(am, s) when the pH became lower. At pH 6, PYO yielded a rate very close to those of PCA and PCN. At pH 5, PYO was more reactive than PCA and PCN, only less reactive than 1-OHPHZ. For reactions with α-Fe_2O_3(s) at pH 5, compared to $Fe(OH)_3$(am, s), phenazine reactivity was more closely correlated with the $E_{1/2}$, and the rates decreased in the order: 1-OHPHZ > PCA ≅ PCN > PYO. 1-OHPHZ, PCA, and PCN exhibited similar area-corrected rates (R_A) with the two (hydr) oxides, but PYO yielded a R_A value about 15 times lower with α-Fe_2O_3(s) than $Fe(OH)_3$(am, s). At pH 7, PYO failed to yield a measurable rate. 1-OHPHZ, PCA, and PCN yielded R_A values 30–50 times lower with α-Fe_2O_3(s) than with $Fe(OH)_3$(am, s). The rates decreased in the order: 1-OHPHZ > PCA ≅ PCN.

To evaluate the pH effect on reaction rate, we constructed a log R_0 versus pH plot for reactions with $Fe(OH)_3$(am, s) and calculated orders with respect to $[H^+]$ as slopes between successive pairs of points (Figure 4). Between pH 7 and 8, 1-OHPHZ, PCA, and PCN all yielded slopes greater than 1. Slopes decreased substantially as the pH decreased. Decreasing the pH from 7 to 6, 1-OHPHZ, PCA, and PCN all yielded slopes nearly half-order. Further decreasing the pH from 6 to 5, 1-OHPHZ and PCA yielded slopes nearly zeoreth-order, indicating an independence of the pH change; PCN yielded a slope of 0.4, indicating a smaller pH dependence than at higher pH values; PYO yielded a slope of 0.6, leading to the strongest pH dependence among all four phenazines. For reactions with α-Fe_2O_3(s), rates at pH 7 were nearly 2 orders of magnitude lower than at pH 5 for all four phenazines.

For a surface redox reaction, the overall rates are often proportional to the extent of adsorption and the rate of electron transfer (30). PCN, PYO, and 1-OHPHZ (oxidized and reduced) are neutral molecules in the studied pH range; hence, their adsorption onto Fe(III) (hydr)oxides is expected to be weak. Although PCA has one negatively charged carboxylate group, its adsorption is again expected to be weak considering the very low surface loading employed here (30). For weakly adsorbed and structural-closely related molecules, higher redox reactivity is often associated with a lower $E_{1/2}$ value, which suggests the rate-limiting step for the overall reaction may be governed by electron transfer. Consistent with what we report for phenazines, a similar trend has been observed with substituted phenols (31). However, adsorption and electron transfer may depend differently on phenazine structure, Fe(III) mineralogy, and pH. These may complicate kinetics such that reaction rates cannot be explained based solely on one property. At pH 5, in contrast to other phenazines, PYO is exceptionally reactive with Fe $(OH)_3$(am, s) but not with α-Fe_2O_3(s), after correcting for surface area differences. This cannot be explained by the surface charge differences either, because pH_{zpc} values of $Fe(OH)_3$(am, s) and α-Fe_2O_3(s) are expected to be similar (mostly reported in the range 7–9 (32)). Another possible confounding factor in rationalizing the reactivity trends we observe is that changes to

mineral surface structure as dissolution takes place are not accounted for either by surface area normalization or by surface charge characteristics. Moreover, compared to other phenazines, oxidized PYO is subject to keto–enol tautomerization, which might contribute to its anomalous behavior. Given these unknowns, it is perhaps not surprising that we observed discernible rates of α-Fe_2O_3(s) reduction at pH 7 by PCA and PCN despite thermodynamic predictions to the contrary. A fuller characterization at the molecular level with respect to factors such as speciation and surface configuration will be necessary to resolve the underlying reaction mechanisms.

Reactions with Oxygen

Cellular production of a phenazine is stimulated by low O_2 tension and by the presence of Fe (III) (17,18). Hence, situations may exist where O_2 and Fe(III) compete to accept electrons from a reduced phenazine. To quantify phenazine reactivity with O_2, we performed experiments employing 5 μM reduced phenazine and 2.0% O_2 (27 μM) at pH 7. We selected 2.0% O_2 instead of air (21% O_2) to mimic natural phenazine production conditions, and also to make sure that the reaction rates would be slow enough to measure. We selected a phenazine concentration several times lower than that of O_2 to obtain pseudo-order kinetics. HPLC analyses of the reaction solutions at their last time points showed a single phenazine peak, indicative of a two-electron oxidation via a reversible pathway (Table 1), ruling out any irreversible degradation. We obtained initial rates by following the decrease in concentration of the reduced phenazine as a function of time (Figure S5, Supporting Information): 63.1 ± 11.2 μM/h with PYO, 36.5 ± 3.2 μM/h with 1-OHPHZ, and 14.4 ± 0.9 μM/h with PCA. PYO, which exhibited the least reactivity toward both $Fe(OH)_3$(am, s) and α-Fe_2O_3(s) at pH 7, was the most reactive phenazine toward O_2. These differences in reactivity are particularly interesting given that PYO production is inhibited when *P. aeruginosa* grows anaerobically but PCA production is not.

Environmental Implications

In this study, we have shown that different phenazines react differently with Fe(III) minerals and molecular oxygen. This is potentially important in environmental contexts where gradients of iron and oxygen occur, such as within biofilms forming on the surface of corroding steel pipelines, from which *Pseudomonas* species have been isolated (33). In addition to forming biofilms on steel, pseudomonads are known to form biofilms on many other substrates, including the lungs of patients with cystic fibrosis (CF) (34). In this context, biofilms have been reported to grow up to > 100 μm in diameter within the mucus covering the lung epithelial cell, where steep O_2 gradients exist and the majority of bacterial cells are thought to live under hypooxic or anaerobic conditions (35) and possibly be iron-limited (36). Although the distribution of phenazines within these biofilms has not yet been measured, phenazine production is known to occur within the CF lung (37); moreover, the pH of *P. aeruginosa* biofilms has been reported to be between 5.6 and 7 (38), consistent with the pH range studied here. In addition, phenazine production is thought to confer a competitive advantage upon pseudomonads colonizing the surfaces of plant roots in the rhizosphere (39), as well as facilitate electron transfer for biofilms growing on the surfaces of electrodes (40). Given that phenazine production is different under different conditions (17,18), we hypothesize that gradients of phenazines themselves may also exist within these biofilms and that their spatial location may correlate with their reactivity. For example, PYO requires molecular oxygen for its production and, as we have shown in this study, PYO is the most reactive phenazine with O_2. In contrast, PCA can be produced under anaerobic conditions and is more reactive with Fe(III) than PYO. Thus, it is tempting to speculate that PYO produced in the upper regions of a biofilm may play an important role as a virulence factor, limiting the growth of other cells in its vicinity (41), whereas deeper in the biofilm where O_2 and iron are limiting, PCA and other phenazines may be more relevant for iron acquisition and/or maintaining intracellular redox homeostasis, as

has been shown in stationary-phase planktonic cultures (6,10,15,42). In addition, given that natural phenazines cover a relatively wide range of the redox spectrum, it is possible that within diffusion-limited environments, such as biofilms (43), redox reactions between different phenazines may facilitate electron transfer over the spatial scale of the biofilm. We are currently developing imaging techniques to test these predictions. Finally, some synthetic veterinary antibiotics (e.g., carbadox and olaquindox) that have been detected in soils (44) share the core redox-active structures of natural phenazines. It will be interesting to explore whether they can shuttle electrons to reduce Fe(III) minerals like their natural analogs.

Supplementary Material

Refer to Web version on PubMed Central for supplementary material.

Acknowledgments

We thank Thomas Hamann for his help with the electrode experiments, Ekaterina Pletneva and Jay Winkler for their help with the oxygen experiments, Michelle Scherer for the gift of the hematite samples, Alan Stone and Newman lab members for stimulating discussions, and four anonymous reviewers for insightful comments. This work was supported by grants to D. K. N. from the Packard Foundation and the Howard Hughes Medical Institute.

Literature Cited

1. Lovley DR. Dissimilatory Fe(III) and Mn(IV) reduction. Microbiol. Rev 1991;55:259. [PubMed: 1886521]
2. Braun V, Killmann H. Bacterial solutions to the iron supply problem. Trends Biochem. Sci 1999;24:104. [PubMed: 10203757]
3. Mehta T, Coppi MV, Childers SE, Lovley DR. Outer membrane c-type cytochromes required for Fe (III) and Mn(IV) oxide reduction in *Geobacter sulfurreducens*. Appl. Environ. Microb 2005;71:8634.
4. Reguera G, McCarthy KD, Mehta T, Nicoll JS, Tuominen MT, Lovley DR. Extracellular electron transfer via microbial nanowires. Nature 2005;435:1098. [PubMed: 15973408]
5. Lovley DR, Coates JD, BluntHarris EL, Phillips EJP, Woodward JC. Humic substances as electron acceptors for microbial respiration. Nature 1996;382:445.
6. Hernandez ME, Kappler A, Newman DK. Phenazines and other redox-active antibiotics promote microbial mineral reduction. Appl. Environ. Microb 2004;70:921.
7. Lies DP, Hernandez ME, Kappler A, Mielke RE, Gralnick JA, Newman DK. Shewanella oneidensis MR-1 uses overlapping pathways for iron reduction at a distance and by direct contact under conditions relevant for biofilms. Appl. Environ. Microb 2005;71:4414.
8. Newman DK, Kolter R. A role for excreted quinones in extracellular electron transfer. Nature 2000;405:94. [PubMed: 10811225]
9. Nevin KP, Lovley DR. Mechanisms for accessing insoluble Fe(III) oxide during dissimilatory Fe(III) reduction by *Geothrix fermentans*. Appl. Environ. Microb 2002;68:2294.
10. Hernandez ME, Newman DK. Extracellular electron transfer. Cell. Mol. Life Sci 2001;58:1562. [PubMed: 11706984]
11. Price-Whelan A, Dietrich LEP, Newman DK. Rethinking “secondary” metabolism: Physiological roles for phenazine antibiotics. Nat. Chem. Biol 2006;2:71. [PubMed: 16421586]
12. Nurmi JT, Tratnyek PG. Electrochemical properties of natural organic matter (NOM) fractions of NOM, and model biogeochemical electron shuttles. Environ. Sci. Technol 2002;36:617. [PubMed: 11878375]
13. Turner JM, Messenger AJ. Occurrence biochemistry and physiology of phenazine pigment production. Adv. Microb. Physiol 1986;27:211. [PubMed: 3532716]
14. Cox CD. Role of pyocyanin in the acquisition of iron from transferrin. Infect. Immun 1986;52:263. [PubMed: 2937736]

15. Dietrich LEP, Price-Whelan A, Petersen A, Whiteley M, Newman DK. The phenazine pyocyanin is a terminal signalling factor in the quorum sensing network of *Pseudomonas aeruginosa*. Mol. Microbiol 2006;61:1308. [PubMed: 16879411]
16. Smolen JM, McLaughlin MA, McNevin MJ, Haberle A, Swantek S. Reductive dissolution of goethite and the subsequent transformation of 4-cyanonitrobenzene: Role of ascorbic acid and pH. Aquat. Sci 2003;65:308.
17. Korth H. Effect of iron and oxygen on formation of pigments in some *Pseudomonas* spp. Archiv Fur Mikrobiol 1971;77:59.
18. van Rij ET, Wesselink M, Chin-A-Woeng TFC, Bloemberg GV, Lugtenberg BJJ. Influence of environmental conditions on the production of phenazine-1-carboxamide by *Pseudomonas chlororaphis* PCL1391. Mol. Plant Microbe In 2004;17:557.
19. Price-Whelan A, Newman DK. unpublished data.
20. Schwertmann, U.; Cornell, RM. Iron Oxides in the Laboratory – Preparation and Characterization. New York: Wiley-VCH; 2000.
21. Komadel P, Stucki JW. Quantitative assay of minerals for Fe^{2+} and Fe^{3+} using 1,10-phenanthroline. 3. A rapid photochemical method. Clays Clay Miner 1988;36:379.
22. Larese-Casanova P, Scherer MM. Fe(II) sorption on hematite: New insights based on spectroscopic measurements. Environ. Sci. Technol 2007;41:471. [PubMed: 17310709]
23. Bard, AJ.; Faulkner, LR. Electrochemical Methods: Fundamentals and Applications. New York: John Wiley; 2001.
24. Elema B. Oxidation-reduction potentials of chlororaphine. Recueil Des Travaux Chimiques Des Pays-Bas 1933;52:569.
25. Muller OH. Oxidation-reduction potentials measured with the dropping mercury electrode IV Polarographic study of α-oxyphenazine. J. Biol. Chem 1942;145:425.
26. Friedheim E, Michaelis L. Potentiometric study of pyocyanine. J. Biol. Chem 1931;91:355.
27. Mann S. Studies on identification and redox properties of the pigments produced by *Pseudomonas aureofaciens* and *P. iodina*. Archiv Fur Mikrobiol 1970;71:304.
28. Jeon BH, Dempsey BA, Burgos WD. Kinetics and mechanisms for reactions of Fe(II) with iron(III) oxides. Environ. Sci. Technol 2003;37:3309. [PubMed: 12966975]
29. Morel, FMM.; Hering, JG. Principles and Applications of Aquatic Chemistry. New York: Wiley; 1993.
30. Wang Y, Stone AT. Reaction of $Mn^{III,IV}$ (hydr)oxides with oxalic acid, glyoxylic acid, phosphonoformic acid, and structurally-related organic compounds. Geochim. Cosmochim. Ac 2006;70:4477.
31. Stone AT. Reductive dissolution of manganese(III/IV) oxides by substituted phenols. Environ. Sci. Technol 1987;21:979.
32. Cornell, RM.; Schwertmann, U. The Iron Oxides—Structure, Properties, Reactions, Occurrences and Uses. Vol. 2nd ed. Weinheim: Wiley-VCH; 2003.
33. Obuekwe CO, Westlake DWS, Cook FD, Costerton JW. Surface changes in mild-steel coupons from the action of corrosion-causing bacteria. Appl. Environ. Microb 1981;41:766.
34. Costerton JW, Stewart PS, Greenberg EP. Bacterial biofilms: A common cause of persistent infections. Science 1999;284:1318. [PubMed: 10334980]
35. Worlitzsch D, Tarran R, Ulrich M, Schwab U, Cekici A, Meyer KC, Birrer P, Bellon G, Berger J, Weiss T, Botzenhart K, Yankaskas JR, Randell S, Boucher RC, Doring G. Effects of reduced mucus oxygen concentration in airway Pseudomonas infections of cystic fibrosis patients. J. Clin. Invest 2002;109:317. [PubMed: 11827991]
36. Zeng AP, Kim EJ. Iron availability, oxygen limitation, *Pseudomonas aeruginosa* and cystic fibrosis. Microbiol.-Sgm 2004;150:516.
37. Finnan S, Morrissey JP, O'Gara F, Boyd EF. Genome diversity of *Pseudomonas aeruginosa* isolates from cystic fibrosis patients and the hospital environment. J. Clin. Microbiol 2004;42:5783. [PubMed: 15583313]

38. Hunter RC, Beveridge TJ. Application of a pH-sensitive fluoroprobe (C-SNARF-4) for pH microenvironment analysis in *Pseudomonas aeruginosa* biofilms. Appl. Environ. Microb 2005;71:2501.

39. Haas D, Defago G. Biological control of soil-borne pathogens by fluorescent pseudomonads. Nat. Rev. Microbiol 2005;3:307. [PubMed: 15759041]

40. Rabaey K, Boon N, Hofte M, Verstraete W. Microbial phenazine production enhances electron transfer in biofuel cells. Environ. Sci. Technol 2005;39:3401. [PubMed: 15926596]

41. Lau GW, Hassett DJ, Ran HM, Kong FS. The role of pyocyanin in *Pseudomonas aeruginosa* infection. Trends Mol. Med 2004;10:599. [PubMed: 15567330]

42. Price-Whelan A, Dietrich LEP, Newman DK. Pyocyanin alters redox homeostasis and carbon flux through central metabolic pathways in *Pseudomonas aeruginosa* PA14. J. Bacteriol 2007;189:6372. [PubMed: 17526704]

43. Stewart PS. Diffusion in biofilms. J. Bacteriol 2003;185:1485. [PubMed: 12591863]

44. Richardson SD. Water analysis: Emerging contaminants and current issues. Anal. Chem 2007;79:4295. [PubMed: 17508722]

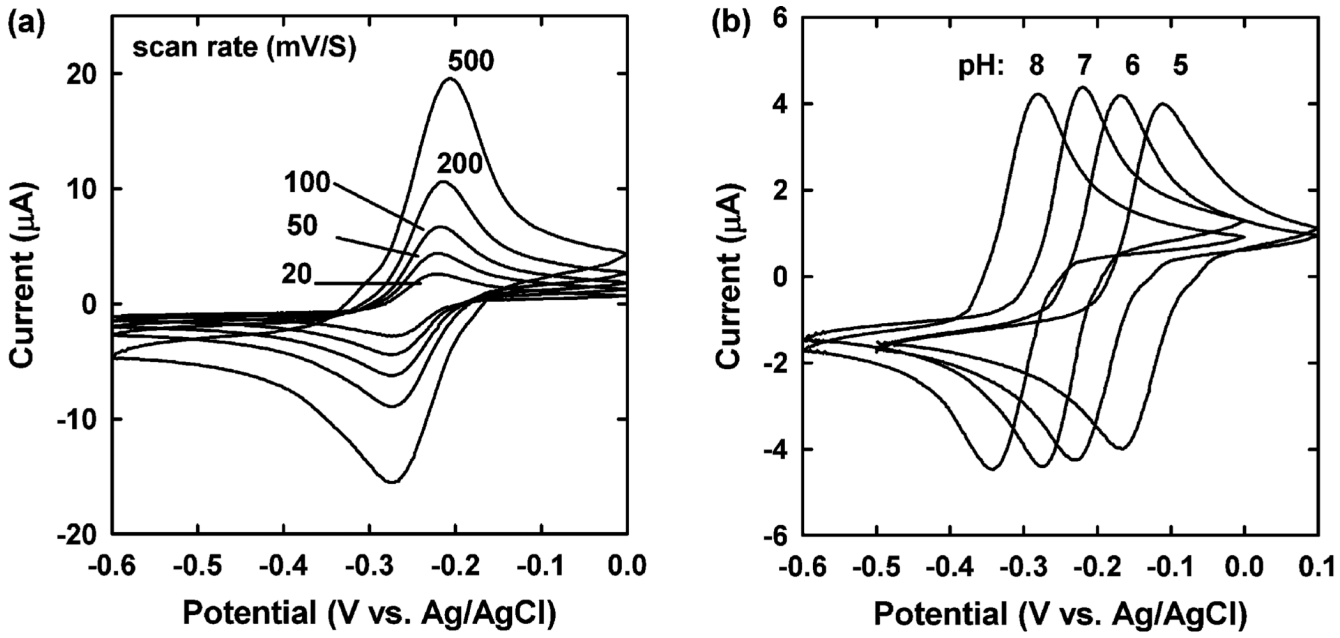

FIGURE 1.

Effects of (a) the voltage scan rate at pH 7 and (b) pH from 5 to 8 on illustrative CVs measured with 821 μM PYO in 0.1 M KCl aqueous solution buffered with 10 mM $CH_3C(O)ONH_4$-MOPS.

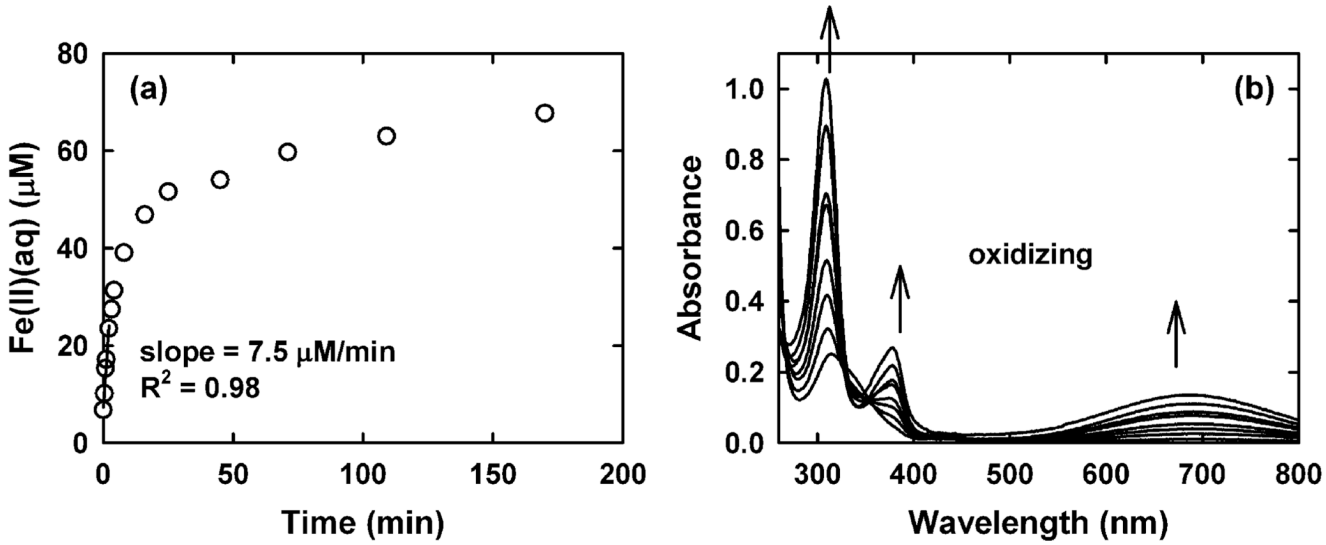

FIGURE 2.

(a) Fe(II)(aq) production as a function of time and (b) UV–visible spectra collected at 0.85, 2.2, 4.2, 16, 45, 109, and 170 min, during the reaction between 100 μM $Fe(OH)_3$(am, s) and 50 μM reduced PYO at pH 6. Arrows indicate peak growth as the reaction progresses.

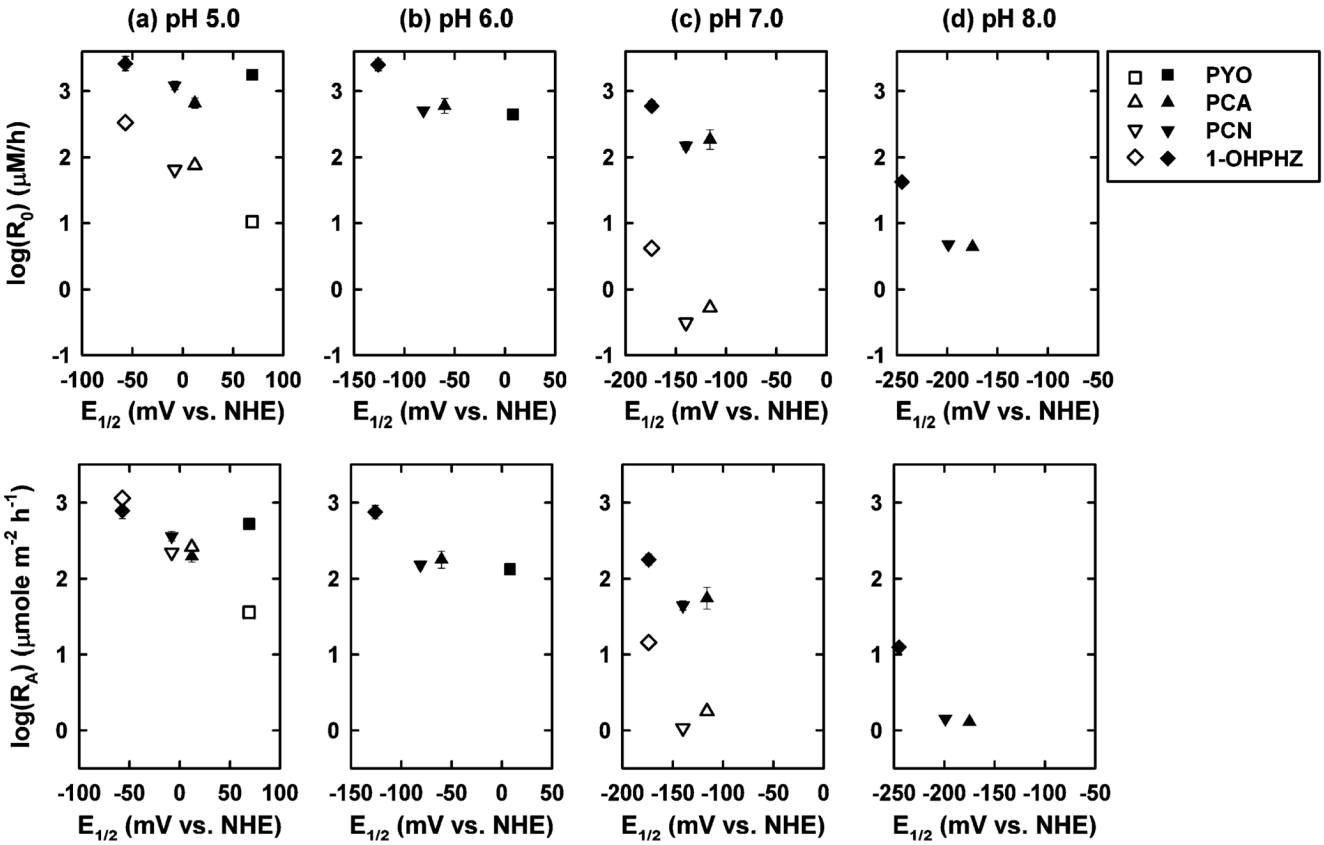

FIGURE 3.

Initial rates with respect to Fe(II)(aq) production for reactions of reduced phenazines with Fe$(OH)_3$(am, s) (filled symbols) and α-Fe_2O_3(s) (open symbols) as a function of the half-wave potential ($E_{1/2}$) of the phenazine redox couples. R_0 values (in the top panels) were derived from the time course plot illustrated in Figure 2a. R_A (in the bottom panels) corrects for differences in surface area loading for the two (hydr)oxides by dividing R_0 by the surface area (in m^2 g^{-1}), the formula weight (in g/mol Fe), and the suspension concentration (in moles Fe/L). All $E_{1/2}$ values were measured in this study and are listed in Table 1, except for PCA and PCN at pH 8, where their $E_{1/2}$ values were derived from eq 1 (see text) using the values measured at pH 7.

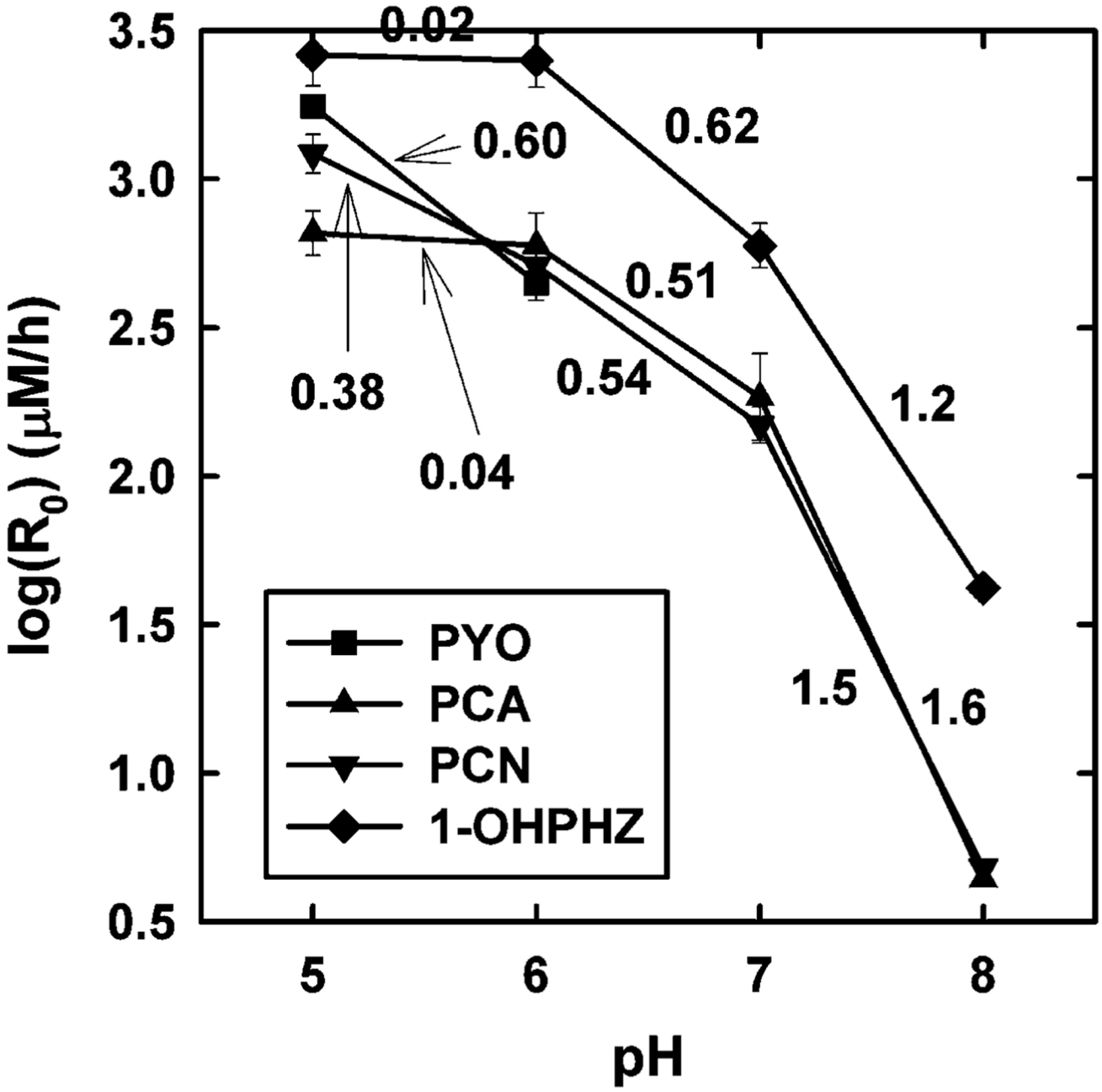

FIGURE 4.
Initial rates with respect to Fe(II)(aq) production as a function of pH. The reported orders with respect to $[H^+]$ were calculated from the straight lines connecting successive pairs of points.

TABLE 1

Chemical structures and half-wave potentials ($E_{1/2}$) of the phenazine redox couples in aqueous solution[a]

Chemical name (abbreviation)	Redox couple involving two-electron transfer	$E_{1/2}$ (vs. NHE) (mV)			
		pH5	pH6	pH7	pH8
pyocyanin (PYO)	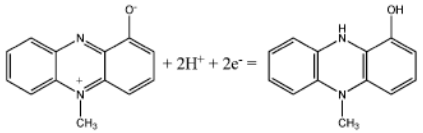	69	8	−40 (−34)[b]	−103
phenazine-1-carboxylate (PCA)	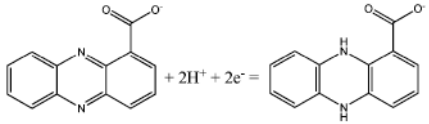	12	−60	−116 (−177)[c]	-
phenazine-1-carboxamide (PCN)	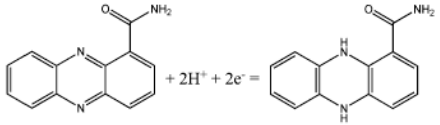	−8	−81	−140 (−115)[d]	-
1-hydroxyphenazine (1-OHPHZ)	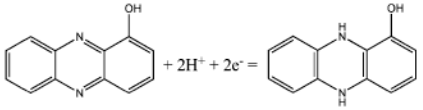	−57	−126	−174 (−172)[e]	−245

[a] Unless otherwise mentioned, $E_{1/2}$ values were measured in aqueous solution in this study. "–", not measureable.

[b] Reference (26).

[c] Reference (27).

[d] Reference (24).

[e] Reference (25).